Part III

INNER DISK OSCILLATIONS

Inner disk oscillations

Tomaso Belloni
Osservatorio Astronomico di Brera, Merate, Italy

Abstract. The RXTE observations of GRS 1915+105 have given a new impulse to the study of spectral and timing properties of the X-ray emission of black hole candidates. At variance with any other known source, GRS 1915+105 shows dramatic changes on time scales as short as a tenth of a second. These changes are associated to marked spectral changes which have been interpreted as changes of the observable inner radius of the accretion disk. I review the existing results and discuss the current evidence for such disk oscillations. Independently of the precise theoretical models, the detailed study of these fast variations can provide an extremely valuable insight on the accretion processes onto black holes. Making use of these results, I compare the properties of GRS 1915+105 with those of other black hole candidates.

Keywords: black hole candidates, microquasar, accretion disk

1. Introduction: black hole candidates

In the recent years, a classification scheme for the X-ray emission of black hole candidates has emerged. From the timing and spectral properties, four separate states (plus the quiescent state for transient systems) have been identified, probably in dependence of the accretion rate level (see van der Klis 1995). Unfortunately, all known persistent sources, Cyg X-1, GX 339-4, LMC X-1 and LMC X-3, show state transitions very rarely, making the accumulation of extensive datasets on different states difficult. Transient systems are more promising, but their transient nature limits the number of states and state transitions that can be observed from one system, and the comparison between different systems is always problematic.

The spectral properties of black hole candidates are usually characterized in terms of a double-component model. The first component is thermal and (when present) contributes mostly to the flux below 10 keV. It is commonly interpreted as emission from an optically thick accretion disk (Mitsuda et al. 1984). The second component is much harder and extends above 10 keV. In its simple form, it can be approximated as a power law, although more sophisticated models are often required (see e.g. Frontera et al. 2000). An attractive feature of the optically thick disk model, the so-called *disk-blackbody*, is that one of its parameters is the value of the inner radius of the accretion disk. Therefore, the application of this model can in principle yield the measurement of this fundamental parameter, although a precise value

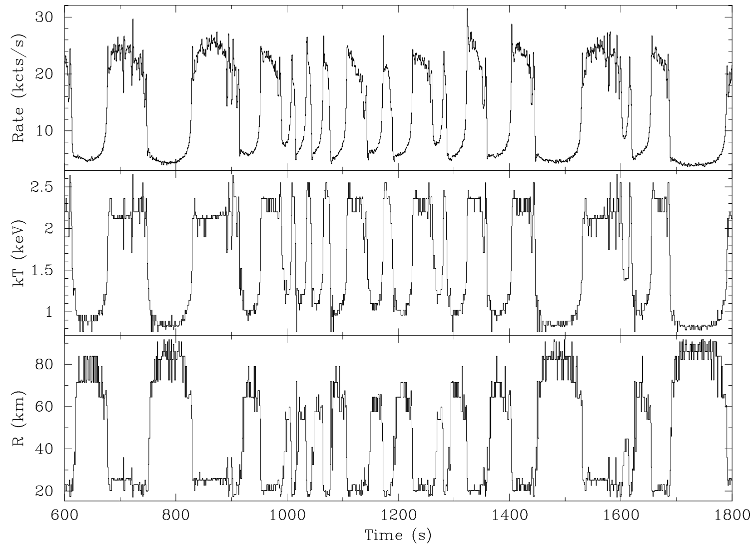

Figure 1. Count rate, inner disk temperature and radius as a function of time of the 1997 Jun 18th of GRS 1915+105 (from Belloni et al. 1997b).

depends on the distance and the inclination of the system. This model became rather popular when a number of black hole systems showed a rather constant inner disk radius, around 20-30 km, despite large changes in accretion rate (see Tanaka & Lewin 1995). Although this model is simplified and leads to an underestimate of the values of the radii, it can detect large variations in the inner radius of the disk (see Merloni, Fabian & Ross 2000).

2. GRS 1915+105: inner disk oscillations

The galactic Microquasar GRS 1915+105 is known to exhibit dramatic variability in the soft (1-20 keV) energy band (see Greiner, Morgan & Remillard 1996; Belloni et al. 2000) and since its appearance in 1992 it has remained active up to the time of writing. This variability is accompanied by strong spectral changes (Greiner, Morgan & Remillard 1996; Belloni et al. 1997a,b; Muno, Morgan & Remillard 1999), providing an ideal system to study spectral transitions in a black-hole candidates: the source is always observable and significant spectral variability is present on very short time scales. At the same time, a complex behavior is observed in the power density spectra of the source (see Rao, this volume). Right: corresponding

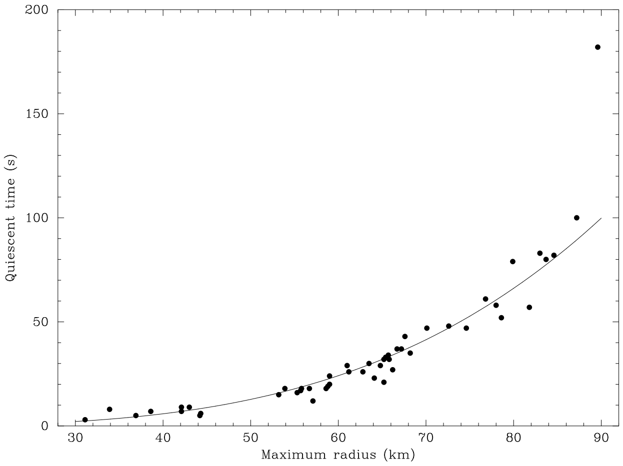

Figure 2. Relation between disk re-fill time and inner disk radius for the same observation shown in Figure 1 (from Belloni et al. 1997b).

Belloni et al. (1997a,b) proposed a model for the observed spectral variations, based on fits to RXTE/PCA data with the approximated spectral shape described above. They interpret the observations as the onset of a thermal-viscous instability, during which the innermost part of the accretion disk becomes unobservable and is slowly refilled from the outer parts. This interpretation is based on the measurement of a variable inner disk radius from energy spectra (see Figure 1) and is supported by the observation of the expected dependence between size of the unstable region and refill time (Figure 2). The observed radius variations are too large to be attributed to spurious effects due to the approximate form of the model. This is what I will refer to as 'inner disk oscillations'. The modeling by these authors was rather qualitative (with the exception of the estimate of the refill time scale), but other authors have developed more accurate models for this process (Szuszkiewicz & Miller 1998, Nayakshin, Rappaport & Melia 2000, Janiuk et al. 2000).

3. Spectral states of GRS 1915+105

Belloni et al. (2000) analyzed a large number of RXTE/PCA observations of GRS 1915+105 and obtained a subdivision of the observed phenomenology into 12 separate classes. From this classification, they identified three basic states, the alternation of which cause all of the observed variability. The three classes, called A, B and C, are shown schematically in Figure 3, which represents a color-color diagram (both colors increase with increasing hardness of the spectrum).

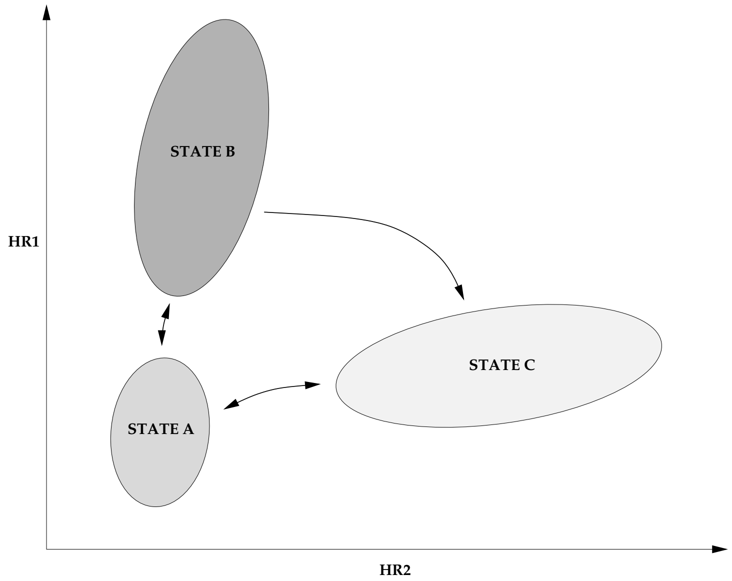

Figure 3. Schematic color-color diagram showing the basic A/B/C states and their observed transitions (from Belloni et al. 2000).

These states correspond to the three states already identified by Markwardt, Swank & Taam (1999). Class B correspond to the "normal" state of a black hole candidate at high accretion rate (the very high state), with an optically thick accretion disk extending down to the last stable orbit and a steep power-law component. State C corresponds to the instability periods: the accretion disk stops at a larger radius than in state B, while the power law component is harder. State A is a new state, not recognized earlier. It corresponds to an accretion disk like in state B, but with a lower temperature, and therefore lower local accretion rate. The relatively fast transition time between A and B is consistent with being the viscous time scale at the innermost stable orbit around the black hole. The observed variability consists of transitions between these three states: all possible transitions between two of the states are observed, with the exception of C to B transitions, of which no example has been found.

There are intervals of time, even as long as a month, when the source is found only in state C. These are the 'plateau' intervals observed in the radio band (see Fender 1999). These are consistent with being long instability intervals, when a large missing inner disk is slowly refilled at a lower external accretion rate (Belloni et al. 2000). On the other hand, there are very fast variations as well. During some observations, variability of a factor of five in 0.1 seconds has been observed, corresponding to fast A–B/B–A transitions (Belloni et al. 2000).

4. Timing properties

It is important to connect what is observed in the time domain and the state transitions described above. As a first step, I consider the three types of QPOs observed in GRS 1915+105:

- 1-10 Hz QPO: (see Rao, this volume). This QPO is only observed during state C. Its central frequency varies systematically with time, count rate and hardness. Since state C is the only state when systematic changes in the inner disk radius are observed, it is natural to associate this oscillation to the inner radius, although often the missing part of the disk is so large that no disk component is observed directly, indicating that the QPO must be related to the power law component.

- 67 Hz QPO: This QPO appears only during state B. Its high and rather constant frequency and its association with a state with small (and possibly constant) inner disk radius also point to a connection to the inner disk radius. It is interesting to note that this QPO is not observed in all state-B intervals, indicating that there must be another parameter involved in its production.

- Low-ν QPO: These oscillations, in the range 10-100 seconds (see Morgan, Remillard & Greiner 1997) *are* the regular transitions between states that are often observed. The instability model provides an interpretation for the variability, but does not cast light on why the light curves are so regular.

There is another important point about the timing properties of the source. Looking at the light curves (see Belloni et al. 2000), one notices not only that their time structure is very complex, but also it often repeats in an almost undistinguishable way, so that all observations can be grouped in twelve classes. As mentioned above, there is no clear explanation for why the structure of the light curves is the observed one. More than this, sometimes even the finest structures of the light curves repeat at a distance of years (see Figure 4). The basic question that need to be answered are: why do the light curves have those complex and repeatable shapes, and why do the light curves have *only* those complex shapes, with only a few possibilities to choose from? Answering these questions could provide crucial information about the accretion phenomenon.

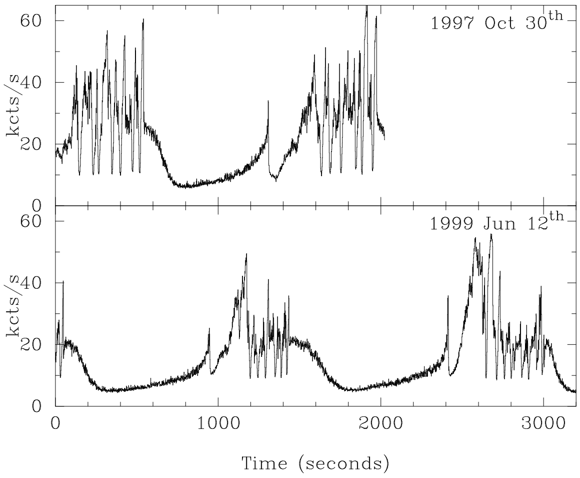

Figure 4. Two PCA light curves of GRS 1915+105 separated by almost two years. The similarity between the two panels, even in some small details, is evident.

5. A unique source?

Another important question is: are there other sources that show the same phenomenology seen here? To this date, the answer is: the C-state events (the instability) are observed only in GRS 1915+105, but A–B transitions have been observed in other systems, namely 4U 1630-47 and GRO J1655-40 (Trudolyubov, Borozdin & Priedhorsky 2000, see Figure 5). Possibly, the dips and the so-called flip-flops seen earlier in GX 339-4 (Miyamoto et al. 1991) are also of the same nature. It seems clear that this type of fast (and often very regular) temperature oscillations are more common among bright black hole candidates, although their origin is still unknown. The question of why the C-state instability is observed only in this source is still basically unanswered. Possibly, this type of instability appears only at very high levels of accretion rate, which would then be reached only by GRS 1915+105. The observation of the same phenomenon in another source would greatly help to understand this issue.

6. Relation to the canonical black hole states

An important point is the comparison between the A/B/C states of GRS 1915+105 and the four canonical black hole states mentioned above. It is tempting to associate state C with the low/intermediate state (hard spectrum flat-top noise and QPO in the power spectrum), state B with the very high state (strong disk component, weaker noise

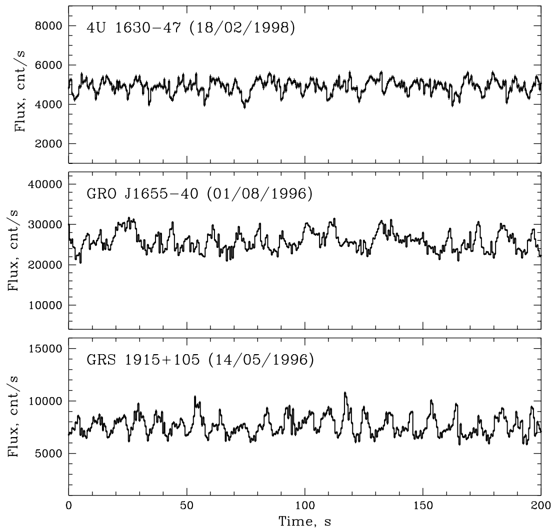

Figure 5. Comparison between selected RXTE/PCA light curves of 4U 1630-47 (upper panel, GRO J1655-40 (middle panel) and GRS 1915+105 (lower panel). From Trudolyubov, Borozdin & Priedhorsky (2000).

level), and the A state with the high state (cooler disk component, low noise level). However, as mentioned above, the instability related to the C state is not observed in other sources. It is more likely that the similarities between the properties of GRS 1915+105 and the canonical black hole states are not indicative of them being the same, but rather of them looking the same. In other words, the onset of the instability in GRS 1915+105 influences the accretion structure in a way that makes it mimic the properties of the canonical states observed in "normal" sources.

7. Inner disk oscillations and radio jet ejection

The X-ray phenomenology described above has been positively linked to the variability observed in the radio band, and major events have been associated to the emergence of superluminal radio jets. This topic is treated by other authors in this volume. Here it is important to stress that the analysis of simultaneous X-ray/radio observations has shown that radio flares seem to be associated only to state C events, and therefore to the inner disk oscillations, while observations containing only states A and B do not correspond to significant radio detections of the source (see Klein-Wolt et al., this volume). However, the presence of this instability has not yet been observed in the other galactic sources showing jet ejection in the radio.

8. Conclusions

GRS 1915+105 is the only source up to now which can provide a large number of spectral transitions, enabling us to study different states of one source without having to wait for years. The most important of these transitions do not involve the canonical states of black hole candidates, but are associated to an instability of the innermost region of an optically thick accretion disk, which causes its inner parts to be evacuated and refilled on the local viscous time scale. Other variations observed in this source can be linked to those observed in other sources, strengthening the connection between this unique system and more conventional ones. On the X-ray side, it is now important to examine the spectral/timing behavior of GRS 1915+105 in more detail (see Migliari, Vignarca & Belloni, this volume), in order to provide a more complete phenomenological picture for further theoretical work. Modeling of the X-ray properties of GRS 1915+105 is at the moment the most promising way to make significant progress in the understanding of accretion onto black holes.

References

Belloni, T., et al., 1997a, ApJ, 479, L145
Belloni, T., et al., 1997a, ApJ, 488, L109
Belloni, T., et al., 2000, A&A, 355, 271
Fender, R.P., et al., 1999, MNRAS, 304, 865
Frontera, F., et al., 2000, ApJ, in press (astro-ph/0009160)
Greiner, J., Morgan, E.H., Remillard, R.A., 1996, ApJ, 473, L107
Janiuk, A., et al., 2000, ApJ, in press (astro-ph/0008354)
Markwardt, C.B., Swank, J.H., Taam, R.E., 1999, ApJ, 513, L37
Morgan, E.H., Remillard, R.A., Greiner, J., 1997, ApJ, 482, 993
Merloni, A., Fabian, A.C., Ross, R.R., 2000, MNRAS, 313, 193
Muno, M.P., Morgan, E.H., Remillard, R.A., 1999, ApJ, 527, 321
Mitsuda, K., et al., 1984, PASJ, 36, 741
Miyamoto, S., et al., 1991, ApJ, 383, 784
Nayakshin, S., Rappaport, S., Melia, F., 2000, ApJ, 535, 798
Szuszkiewicz, E., Miller, J.C., 1998, MNRAS, 298, 888
Tanaka, Y., Lewin, W.H.G, 1995, in "X-ray binaries", Cambridge Univ. Press, p126
Trudolyubov, S.P., Borozdin, K.N., Priedhorsky W.C., 2000, MNRAS, in press (astro-ph/9911345)
van der Klis, M., 1995, in "X-ray binaries", Cambridge Univ. Press, p252

On the nature of the microquasar `V4641 Sagittarii` *

S. Chaty (`s.chaty@open.ac.uk`)
Department of Physics and Astronomy, The Open University, United Kingdom

I.F. Mirabel
Service d'Astrophysique, CEA/Saclay, France & IAFE/Conicet, Argentina

J. Martí
Departamento de Física, Escuela Politécnica Superior, Universidad de Jaén, Spain

L.F. Rodríguez
Instituto de Astronomía, Campus UNAM, Morelia, Michoacán 58190, México

Abstract. We present photometric and spectroscopic optical and near-infrared (NIR) observations taken during the outburst on September 1999 of the source V4641 Sgr = SAX J1819.3-2525 (in't Zand et al., 2000) = XTE J1819-254 (Markwardt et al., 1999). We show that our observations suggest a distance between 4 and 8 kpc, the spectral type of the companion star being constrained between B3 and A2 V, making the system a High Mass X-ray Binary System (HMXB). In view of the radio and optical/NIR observations, it is possible that the ejecta of the source interacted with the surrounding medium of the source.

Keywords: V4641 Sgr, X-ray:stars, infrared:stars

1. Introduction

The source V4641 Sgr = SAX J1819.3-2525 = XTE J1819-254 attracted considerable attention after the detection of a giant optical outburst on 1999 September 15.7 UT, from the magnitudes 14.0 to 8.8 in the V-band (Stubbings, 1999). The X-ray source flared, from 1.6 to 12.2 Crab in the 2-12 keV X-rays on 1999, September 14th, as observed by XTE, through a brief but dramatic eruption, its position being coincident with the optical transient (Smith et al., 1999). Less than 10 hours later, the source was fainter than 50 mCrab.

The VLA detected on Sep. 16.0 UT a strong radio source at 0.4 Jy at the position of the variable star. An elongation was extending $0.25''$ between 0.6-1.2 day after the X-ray flare, and at the same position on 17.9, 22 and 24 UT. This allows to classify the source as a new

* Based on observations collected at the European Southern Observatory, Chile. S.C. thanks Rob Hynes for having alerted him to this new flaring source on September 1999, and Bob Hjellming for the communications he gave on the radio observations. S.C. is very grateful to the ESO/NTT team staff for their availability and skills. S.C. acknowledges support from grant F/00-180/A from the Leverhulme Trust. IFM acknowledges partial support from Conicet/Argentina.

microquasar (Hjellming et al., 2000). A detailed study of this source and details on the observations are reported in Chaty et al. (2001).

2. Observations and results

The optical observations were performed with the NTT telescope and the instrument EMMI RILD. We imaged the source in V, R, I and Z filters, and took some spectra with the grism #1. The infrared observations were performed with the NTT and the instrument SOFI through the filters J, H and Ks, with an exposure time of 15 min. The optical and infrared lightcurves and the J-Ks color during the outburst are reported in Figure 1. In the optical, after the big outburst there was still some flaring activity through 0.5 mag in V, R, I with no significant change in the colors. There was also some flaring activity in NIR through 1 mag in J and K, with a significant change in the J-Ks color during the post-outburst stage (between 2 and 5 days after the giant burst). This suggests an increased K-contribution compared to J, either due to the emission of a jet, the appearance of heated dust, or even by the interaction with the interstellar medium.

We report the normalized optical spectra offset in intensity to get an easier reading in Figure 2. On a timescale of one day, the lines were changing from emission to absorption. All the Balmer serie is visible: Hα, β, γ, δ, ϵ, ζ... The Hα emission line is extraordinarily strong: one day after the outburst, its equivalent width was $\sim 100\AA$, with a FWZI of ~ 6700 km s^{-1} and a blue wing. There was also a strong He I 5876$\AA$. The Na-D gives E(B-V) = 0.25 implying $N(\mathrm{H}) = 0.13 \times 10^{22}$ cm^{-2}. The strong variability of the lines and the blue continuum suggest the emission from an accretion disk, or of a corona, with accretion of matter onto a compact object with a high-velocity wind component (~ 6000 km s^{-1}), also perhaps the presence of a cocoon or a jet.

3. Discussion

Taking the magnitudes at the faintest stage of the source in the optical and NIR wavelengths, we plotted them on a color-magnitude diagram (Figure 3). We also plotted three different absorptions, corresponding respectively to 0.05, 0.1 and 0.15×10^{22} cm^{-2}, and different distances of the source, from 1 to 10 kpc. We can see that the distance is constrained to $4 < d < 8$ kpc in order to have a spectral stellar type consistent with the stars of our Galaxy. This location on the color-magnitude diagram suggests that the spectral type of the companion star of the binary system is only consistent with an early type main sequence star B3 - A2 V. Therefore the mass is constrained between 2 < M < 10 $M_{\odot}$, suggesting that it is a high-mass X-ray binary. This is consistent with optical spectra in quiescence, taken by Orosz et al. (2000), who derived a stellar spectral type of A2 V at a distance of 6.1 kpc.

If the elongation seen in the radio was a moving component, the proper motion is between $224 < \mu < 788$ mas/d depending on the exact time of the ejection. In the following we will assume that this is the approaching (brighter) condensation with $\mu_a = 500$ mas/d. Since $D \leq \frac{c}{\sqrt{\mu_a \mu_r}}$ and from our results $D \geq 4$ kpc, we conclude that the apparent velocity in the plane of the sky would be strongly superluminal, v_a of the order of 12. However, no movement of this elongation was detected between Sept. 16.02 and 24.1 UT, suggesting an interaction with surroundings at $0.25'' \geq 1.5 \times 10^3$ AU at the distance of 6 kpc. This is possible if the ejections began to take place 10 days before the radio detection e.g. on September, 8^{th}, and we can see from Figure 3 that the source was already active at this date. It seems therefore that the activity of this source was not as sporadic as we could have thought at the beginning. Indeed, *RXTE* could detect this source during 270 days before the outburst (in't Zand; Markwardt, private communications).

References

Chaty, S., Mirabel, I.F., Martí, J. and Rodríguez, L.F.:2000, 'On the nature of the microquasar V 4641 Sagittarri', *Proceedings of the 4th INTEGRAL workshop* **Vol. ESA-SP**.

Hjellming, R.M., Rupen, M.P., Mioduszewski, A.J. et al.:2000, 'Light Curves and Radio Structure for the September 1999 Transient Event in V4641 Sagittarii(=XTE J1819-254=SAX J1819.3-2525)', *ApJ* **Vol. 195**, pp. 13403

in't Zand, J.J.M., Kuulkers, E., Bazzano, A., Cornelisse, R., Cocchi, M., Heise, J., Muller, J.M., Natalucci, L., Smith, M.J.S., Ubertini, P.:2000 'BeppoSAX observations of the nearby low-mass X-ray binary and fast transient SAX J1819.3-2525', *A&A* **Vol. 357** pp. 520–526

Markwardt, C.B., Swank, J.H., Marshall, F.E.:1999 'XTE J1819-254, XTE J1743-363, XTE J1710-281, XTE J1723-376', *IAU Circ.* **7120**

Orosz, J.A., Kuulkers, E., van der Klis, M., McClintock, J.E., Jain, R.K., Bailyn, C.D., Remillard, R.A.:2000 'V4641 Sagittarii', *IAU Circ.* **7440**

Smith, D.A., Levine, A.M., Morgan E.H.:1999 'GM SAGITTARII AND SAX J1819.3-2525 = XTE J1819-254', *IAU Circ.* **7253**

Stubbings, R.:1999 'GM SAGITTARII AND SAX J1819.3-2525 = XTE J1819-254', *IAU Circ.* **7253**

Address for Offprints: Department of Physics and Astronomy, The Open University, Walton Hall, MK7 6AA, Milton Keynes, United Kingdom

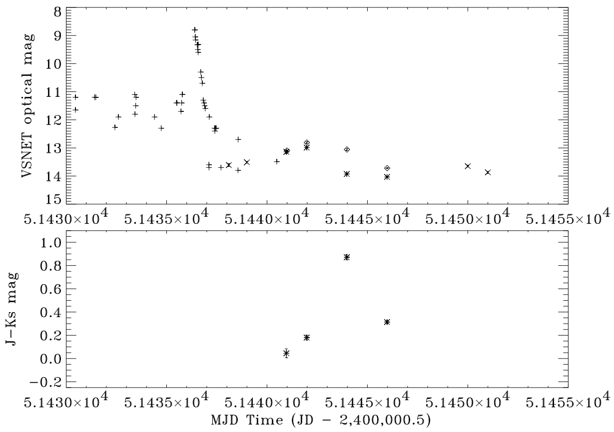

Figure 1. Top: +:VSNET, x:V, *:J, diamond:Ks magnitudes). Bottom: J-Ks color.

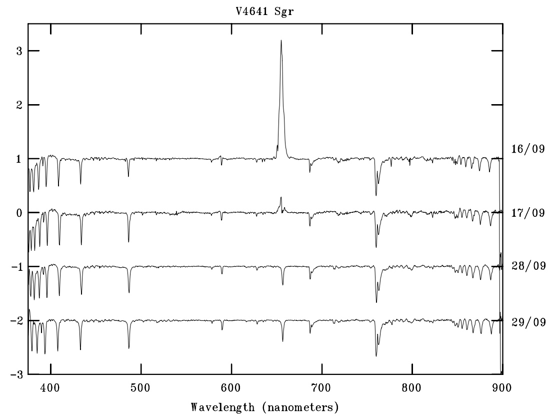

Figure 2. Normalized and offset optical spectra.

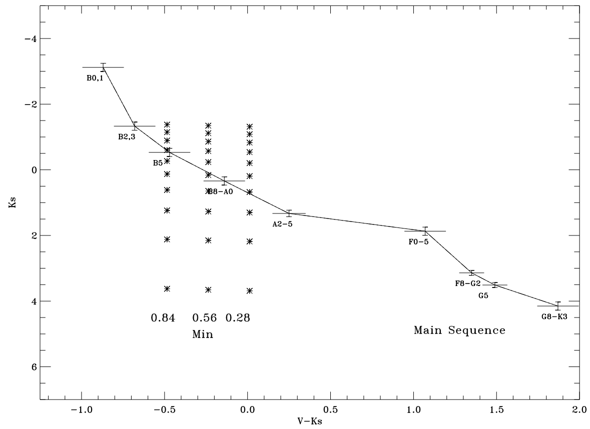

Figure 3. Color-magnitude [V-Ks,Ks] diagram. *: Min magnitudes of V4641 Sgr.

Numerical simulations of the accretion-ejection instability

S. E. Caunt and M. Tagger
DSM/DAPNIA/Service d'Astrophysique (CNRS URA 2052), C.E.A. Saclay, 91191 Gif sur Yvette, France

Abstract. The Accretion-Ejection Instability (AEI) is explored numerically using a global 2d model of the inner region of a magnetised accretion disk. The disk is initially currentless but threaded by an external vertical magnetic field created by external currents, and frozen in the flow. In agreement with the theory a spiral instability, similar in many ways to those observed in self-gravitating disks, but driven by magnetic stresses, develops when the magnetic field is close to equipartition with the disk thermal pressure. The present non-linear simulations give good evidence that such an instability can occur in the inner region of accretion disks.

Keywords: magnetohydrodynamics, instabilities, accretion disk

1. Introduction

The accretion-ejection instability (AEI) (Tagger & Pellat (1999); see also Varnière et al., Rodriguez et al., and Tagger et al., this workshop) can occur close to the inner edge of a magnetised accretion disk when the plasma beta (the ratio of gas to magnetic pressures) is around unity. The instability appears, if the magnetic field decreases outwards sufficiently fast, as a spiral wave of low azimuthal wavenumber, made unstable through the interaction with a Rossby vortex (associated with the gradient of vorticity) which it generates at its corotation radius.

We have undertaken numerical simulations, with a setup optimised according to our previous knowledge of the AEI. We consider an infinitely thin disk threaded by a moderate vertical magnetic field: this is justified by the properties of the AEI, which are essentially constant vertically across the disk (unlike the magneto-rotational instability (Balbus & Hawley, 1991) for which vertical modes are required). The disk is embedded in vacuum and, in order to separate different physical effects, we consider here only configurations where initially the equilibrium magnetic field is due to external currents. Starting with small scale initial random fluctuations in the fluid velocity, the simulations show large-scale spiral perturbations evolving in the disk, and corresponding to the expected properties of the AEI.

The following sections present the essentials of the model, basic results and conclusions. More detailed discussions of these are covered elsewhere (Caunt & Tagger, 2000).

2. The model

Under the assumption, valid for the physics of the AEI, that perturbations are essentially independent of z in the disk, we integrate vertically the standard MHD equations (momentum, continuity, induction) describing the fluid motion in a disk around a central object. We thus solve for the 2d (r, ϕ) evolution of the fluid properties (surface density, velocity, magnetic field) averaged over z. A conservative scheme of the type described by Stone & Norman (1992) is used to ensure that mass, angular momentum and magnetic flux are conserved to numerical precision throughout the simulation.

We assume that the disk is threaded by a poloidal magnetic field which is symmetric about the midplane, hence purely vertical at $z = 0$. In the vacuum surrounding the disk the magnetic field can be described by a magnetic potential which, in turn, results from perturbed currents in the disk. It can thus be calculated from a Poisson equation, similar to the one describing the gravitational potential of a self-gravitating disk, but whose source is the vertical component of the magnetic field at the disk surface (rather than density in the gravitational case). Currents within the disk can be derived from the jump in the horizontal component of the field across the disk. Hence magnetic stresses can be included in an otherwise purely hydrodynamic model.

We assume that the central object has a mass of $M = 10M_\odot$ and the disk extends from between $r = 1,000\,\mathrm{km}$ to $r = 50,000\,\mathrm{km}$ with a constant aspect ratio of $\epsilon = 0.1$. We use a logarithmic radial grid which allows us to get a better resolution in the inner region of the grid, where it is necessary, and to model a very large radial extent of the disk. It also has the added advantage that unwanted effects of the boundary condition at the outer radius of the simulation are avoided (waves are damped more effectively as they approach the outer radius).

3. Results

The results presented here are aimed at illustrating certain properties of the instability as determined by linear theory, specifically the growth rate/magnitude of instability for different field strengths and development of the spiral wave and Rossby vortex.

Figure 1 shows the evolution of the rms velocity within the disk for values of $\beta = 0.1$, 0.5, 1.0, 5.0 and 10.0. As is shown, the perturbed velocity grows rapidly for $\beta = 0.5$ and $\beta = 1.0$, exceeding the initial random noise after approximately 10 orbits. The growth is approximately exponential during this time. For the other values of β we see

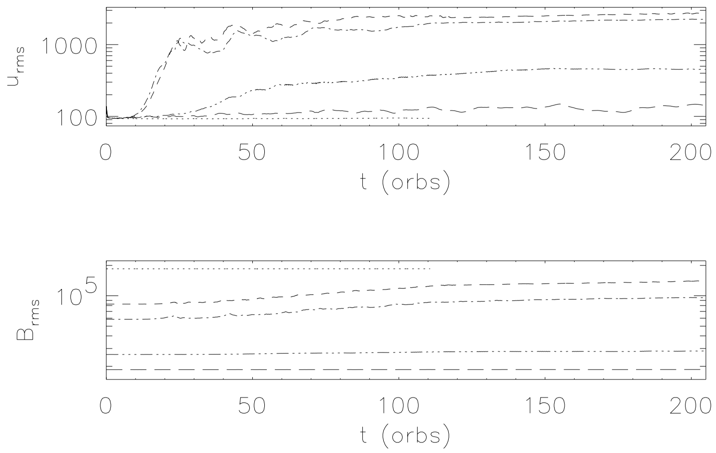

Figure 1. Comparison of the evolution of the instability for different values of the initial β. Values of $\beta = 0.1$, 0.5, 1.0, 5.0 and 10.0 are shown as dotted, dot-dashed, dashed, tripple-dot-dashed and long-dashed lines respectively. Time is given in units of the orbital time at the inner radius. The plots show the evolution of (top) the rms velocity, and (bottom) the rms magnetic field.

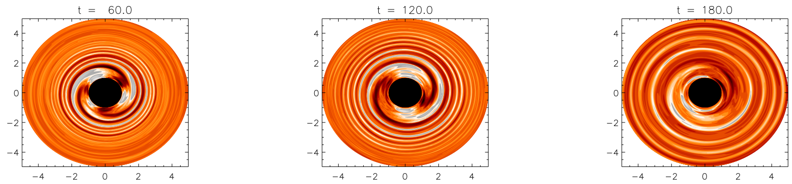

Figure 2. Plots of the spiral structure in the inner region of the disk at times $t = 60$, 120 and 180 orbits. Starting from initially random fluctuations at $t = 0$, the disk has clearly developed 3-armed followed by 2-armed and finally 1-armed spirals.

very little action in comparison. The $\beta = 0.1$ and $\beta = 10.0$ cases are virtually stable with the $\beta = 5.0$ being somewhat more active but failing to achieve the same amplitude as the most unstable cases. This run is still interesting to observe as the growth of the instability is slower and the evolution of the spiral wave is somewhat cleaner.

The evolution of the instability into a well developed spiral wave is best seen for the $\beta = 5.0$ case. Figure 2 shows the different number of spiral arms that occur over time (plotted is the radial velocity): initial random perturbations develop to $m = 3$, $m = 2$ and $m = 1$ spiral structures, as the magnetic flux is advected toward the central region. The transition is generally through a mixture of these for all values

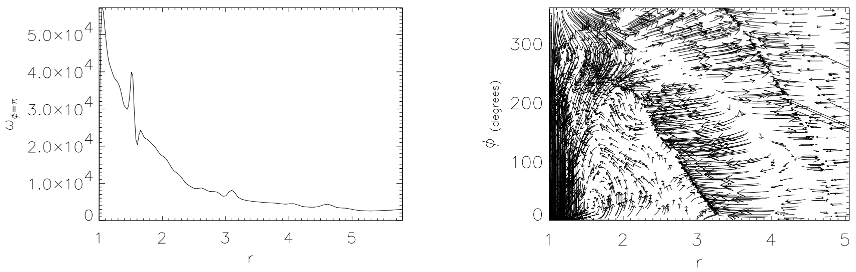

Figure 3. (left hand): Vorticity in the inner region of the accretion disk. (right hand): The velocity field within the disk in Cartesian projection. The vortex is clearly visible around $r \sim 1.5$.

of unstable β. For the more active values ($\beta = 0.5$ and $\beta = 1.0$) the transition is much quicker and always ends up with $m = 1$.

The AEI relies on the existence of a Rossby vortex generated at corotation. Figure 3a shows the radial variation of vorticity in the disk. Clearly shown is a discontinuity close to the inner radius. The velocity field, shown in Figure 3b clearly shows that the fluid flow contains a vortex at the same radius. This is a good indication that a Rossby vortex has indeed been generated at corotation.

4. Conclusions

Using this model we have shown the essential features predicted by linear theory of the AEI. We have seen that the instability is clearly strongest for field strengths of the order of equipartition, and leads to the development of low azimuthal wavenumber spiral waves and a Rossby vortex.

Future work will link in the third type of wave (namely the vertical emission of Alfvén waves) from which the formation of winds and jets is believed to be possible.

References

Balbus, S. A., & Hawley, J. F. 1991, ApJ, 376, 214
Caunt, S. E., & Tagger, M. 2000, submitted to A&A
Stone, J. M., & Norman, M. L. 1992 ApJS, 80, 753
Tagger, M., & Pellat, R. 1999, A&A, 349, 1003

Trapped Disk Oscillations and Stable QPOs in Microquasars

Xue-Bing Wu[1,2]
[1] *Max-Planck-Institut für Astrophysik, Karl-Schwarzschild Str. 1, D-85741 Garching, Germany*
[2] *Beijing Astronomical Observatory, Chinese Academy of Sciences, Beijing 100012; CAS-PKU Joint Beijing Astrophysical Center, Beijing 100871, China*

Abstract. The observed quasi-periodic oscillations (QPOs) in low-mass X-ray binaries have been suggested to be probably related to the characteristic oscillation modes in the inner part of a relativistic accretion disk. In this paper we study the trapped feature of these oscillation modes by considering the radial perturbations and viscosity effects. We find that the trapped oscillations are amplified significantly when the viscosity parameter increases and the trapped size varies when the radial wavenumber and Mach number change. Our results support that the stable hundred-hertz QPOs and their low fractional rms amplitudes found in two Galactic microquasars may be explained by some trapped non-damping oscillation modes in the inner part of accretion disks around rotating black holes.

Keywords: accretion, accretion disk, black hole physics, X-ray:stars

1. Introduction

In recent years, hundred-hertz QPOs have been observed in several black hole X-ray binaries with *RXTE* satellite. These high-frequency QPOs are probably similar to the kilohertz QPOs observed frequently in a dozen neutron star low-mass X-ray binaries. However, the high frequency QPOs in two Galactic microquasars, GRO J1655-40 and GRS 1915+105, are very stable in frequency at 300 Hz and 67 Hz respectively (Morgan, Remillard & Greiner 1997; Remillard *et al.* 1999). These stable QPOs have also very low fractional rms amplitude ($\sim$ 1%). Theoretical models involving frame-dragging (Cui, Zhang & Chen 1998), diskoseismic g-mode (Nowak *et al.* 1997), and periastro precession (Stella, Vietri & Morsink 1999) have been proposed to explain these stable QPOs. But the origin of them is still uncertain.

Recently Psaltis & Norman (2000; hearafter PN) suggested that the observed QPOs in X-ray binaries may be related to the strong resonances peaked at some characteristic oscillation frequencies in the inner part of accretion disks. However, they introduced a simplified term for angular momentum transfer and did not discuss the damping and growth rates of oscillation modes. It is also important to check if some of these modes can be trapped in the inner disk and if the low fractional rms amplitude of QPOs observed in two microquasars can be explained by the trapped feature of oscillation modes.

2. Non-damping Oscillation Modes in Accretion Disk

The basic equations of a geometrically thin accretion disk are the same as those in PN except that the viscosity term in the angular momentum equation is now expressed as: $N_\phi = (1/\rho r)\partial(\nu \rho r^3 d\Omega/dr)/\partial r$. The viscosity is assumed to be described by the usual α prescription, namely, $\nu = \alpha c_{\rm s} H = \alpha c_{\rm s}^2/\Omega$. Like in PN, we consider the general relativistic effects in an approach to specify the the gravitational potential ψ through the dependences of angular velocity (Ω), radial and vertical epicyclic frequencies (κ and $\Omega_\perp$) on the mass, radius and the spin parameter of the central object. We consider small perturbations to all physical quantities in the form of $Q = Q_0 + \delta Q e^{i(\omega t - kr - m\phi)}$, where k and m are radial and azimuthal wavenumbers. We also assume that the perturbations do not alter the local sound speed and the disk is isothermal in the vertical direction. Under the local approximation $kr >> 1$, we can obtain four perturbed equations and derive the dispersion relation as

$$\bar{\sigma}^4 + \alpha\epsilon^2\bar{\sigma}^3 + (\bar{\kappa}^2 + \epsilon^2 + n\bar{\Omega}_\perp^2)\bar{\sigma}^2 - \epsilon[m\frac{H}{r}(\frac{\bar{\kappa}^2}{2} - 2) + 2\alpha\epsilon(\frac{\bar{\kappa}^2}{2} - 2) - \alpha\epsilon^3 - n\epsilon\bar{\Omega}_\perp^2]\bar{\sigma} + n\bar{\kappa}^2\bar{\Omega}_\perp^2 = 0. \quad (1)$$

Here we have defined $\bar{\sigma} = i(\omega - ku_r - m\Omega)/\Omega$, $\bar{\kappa} = \kappa/\Omega$, $\bar{\Omega}_\perp = \Omega_\perp/\Omega$, and $\epsilon = kH$. The value of n represents the number of nodes of the oscillations in the vertical direction.

By solving the dispersion relation (1), we found that the characteristic frequencies of oscillation modes depend on the radial wavenumber and radius significantly but are nearly independent of the viscosity. However, the growth (or damping) rates of these modes depend strongly on the viscosity. According to their non-damping feature, we found that the most possible oscillation modes in the disk are the acoustic modes with approximate frequencies of $ku_r \pm \sqrt{\kappa^2 + k^2 c_{\rm s}^2}$ (in the case of $m = 0$ and $n = 0$) and $ku_r + \Omega \pm \sqrt{\kappa^2 + k^2 c_{\rm s}^2}$ (in the case of $m = 1$ and $n = 0$), neutral modes with frequency of ku_r (in the case of $m = 0$ and $n = 0$) and $ku_r + \Omega$ (in the case of $m = 1$ and $n = 0$), and the corrugation modes with approximate frequencies of $ku_r + \Omega \pm \Omega_\perp$ (in the case of $m = 1$ and $n = 1$). In Figure 1 we show the dependences of oscillation frequencies of all non-damping modes on the disk radius and black hole spin parameters. Note that the lower-frequency acoustic modes and the lower-frequency corrugation mode are trapped in the inner part of

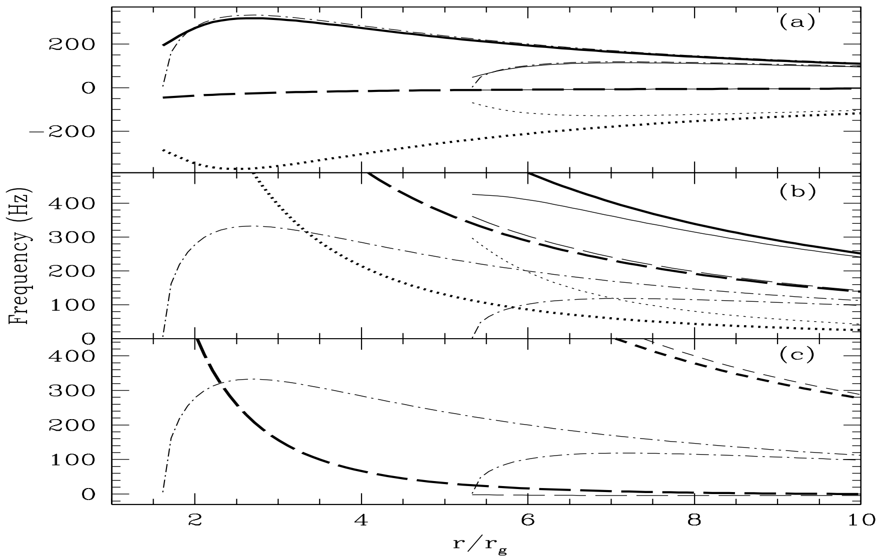

Figure 1. Oscillation frequencies of non-damping modes when $kH = 0.1$ and $|u_r|/c_s = 0.3$. The weighted and light lines represent the cases with black hole spin parameter $a_* = 0.98$ and 0.2. The panel (a), (b) and (c) correspond to (m, n)=(0, 0), (1, 0) and (1,1). In (a) and (b) the solid, dotted and dashed lines represent two acoustic modes and the neutral mode. In (c) the long and short dashed lines represent two corrugation modes. The dot-dashed lines show the radial epicyclic frequencies. The black hole mass was taken to be $7M_{\odot}$and r_g was defined as GM/c^2.

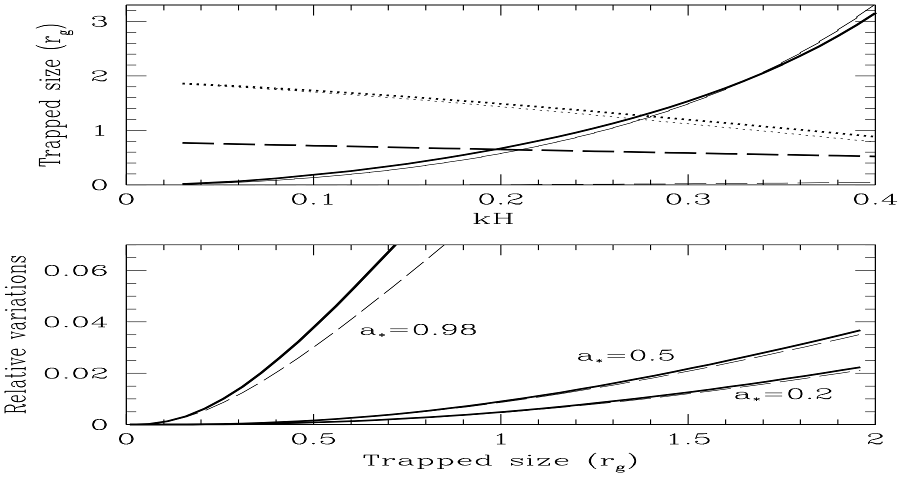

Figure 2. Upper panel: Trapped sizes of three oscillation modes. The solid, dotted and dashed lines represent the lower-frequency acoustic modes in the cases of (m, n) =(0,0) and (1,0), and the lower-frequency corrugation mode in the case of (m, n)=(1,1). The weighted and light lines correspond to the cases with $a_* = 0.98$ and 0.2. Lower panel: Relative variations caused by the trapped oscillations. The solid and dashed lines correspond to the cases with accretion rate of $10^{17} g/s$ and $10^{18} g/s$.

accretion disks since $\omega^2 > \kappa^2$. The trapped sizes of these modes depend significantly on the radial wavenumber, Mach number and black hole spin parameter. The relative luminosity variations caused by the oscillations in the trapped area may be estimated using the expression of local flux emitted from a relativistic accretion disk. These relative variations may be comparable to the observed fractional rms magnitudes if the X-ray luminosity variations are caused by the disk oscillations in the trapped area. In Figure 2 we show the trapped sizes of the oscillation modes and the relative luminosity variations.

3. Conclusion

RXTE observations on GRO J1655-40 have shown 300 Hz QPOs with $\sim 1\%$ rms magnitude. If this stable QPO originates from the trapped disk oscillations, from Figures 1 and 2 we see that it may be explained by either the lower-frequency acoustic mode in the case of $m = 1$ and $n = 0$ or the lower-frequency corrugation mode in the case of $m = n = 1$ and $a_* \sim 0.9$. However, the rapidly spinning black hole is more favored to explain the high QPO frequency. The unambiguous determinations of the inner disk radius and the black hole spin are still needed to confirm this explanation. Further studies on the origin of low-frequency QPOs and their correlation with high-frequency QPOs, as well as the correlation between spectral and temporal properties, will help us to understand more clearly the origin of stable QPOs in microquasars.

References

Cui, W., Zhang, S.N., Chen, W. Evidence for frame-dragging around spinning black holes in X-ray binaries, *Ap. J.* 492:L53-57, 1998

Morgan, E.H., Remillard, R.A., Greiner, J. RXTE observations of QPOs in the black hole candidate GRS 1915+105, *Ap. J.* 482:993-1010, 1997

Nowak, M.A., Wagoner, R.V., Begelman, M.C., Lehr, D.E. The 67 Hz feature in the black hole candidate GRS 1915+105 as a possible "diskoseismic" mode, *Ap. J.* 477:L91-94, 1997

Psaltis, D., Norman, C. On the origin of quasi-periodic oscillations and broad-band noise in accreting neutron stars and black holes, *Ap. J.* in press (astro-ph/0001391)

Remillard, R.A., Morgan, E.H., McClintock, J.E., Bailyn, C.D., Orosz, J.A. RXTE observations of 0.1-300 Hz quasi-periodic oscillations in the microquasar QGO J1655-40, *Ap. J.* 522:397-412, 1999

Stella, L., Vietri, M., Morskink, S.M. Correlations in the quasi-periodic oscillation frequencies of low-mass X-ray binaries and the relativistic precession model, *Ap.J.* 524:L63-66, 1999

Spectra of thermally unstable slim discs

Ewa Szuszkiewicz
Institute of Physics, University of Szczecin, Szczecin, Poland
Toruń Centre for Astronomy, Nicolaus Copernicus University, Toruń, Poland
Dipartimento di Fisica "Galileo Galilei", Università degli Studi di Padova, Italy
International School for Advanced Studies, SISSA, Italy

Roberto Turolla
Dipartimento di Fisica "Galileo Galilei", Università degli Studi di Padova, Italy

Luca Zampieri
Dipartimento di Fisica "Galileo Galilei", Università degli Studi di Padova, Italy

Abstract. Thermal instability driven by radiation pressure might be relevant for intrinsically bright accreting sources. The most promising candidate where this instability seems to be at work is one of the two known galactic superluminal sources, GRS 1915+105 (Belloni et al. 1997). In spite of being of relevance, this scenario has not yet been confirmed by proper time-dependent modelling. Non-linear time-dependent calculations performed by Szuszkiewicz and Miller (1998) show that thermally unstable discs undergo limit-cycle behaviour with successive evacuation and refilling of the central parts of the disc. This evolution is very similar to the one proposed by Belloni et al. (1997) in their phenomenological model. Further investigations are needed to confirm the thermal instability being operational in this source. First of all the spectra emitted from the disc during its evolution should be calculated and compared with observations. Here such spectra are computed assuming local blackbody emission from the best studied transonic disc model.

Keywords: accretion disk, thermal instability, spectra

1. Limit-cycle behaviour of accretion flows

The simplest disc model which properly describes physical conditions around black holes is a transonic (slim) accretion disc. It is an axisymmetric, vertically integrated, non-self-gravitating, differentially rotating fluid configuration. The assumption about self-gravity being negligible defines the outer edge of the disc and the requirement that the radial velocity equals the local sound speed somewhere in the disc, and then exceeds it, determines its radial structure. Once the mass, M, of the central black hole, accretion rate, $\dot{M}$, and viscosity coefficient α are specified the structure of the stationary disc is uniquely determined. However, such a disc might be subject to secular, thermal and pulsational instabilities. Here we focus on the thermal instability in which a temperature perturbation out of the equilibrium is enhanced by thermal processes. Moreover, we consider the thermal instability which is triggered by one particular mechanism, namely by the radiation pressure. The possibility that a global instability might develop in this model was indicated by the results of a local stability analysis. In the temperature - surface density diagram the sequence of equilibrium models forms a characteristic S-shape curve. Such curves reflect the possibility of a transition between low and high accretion rate states, associated with an increase of the temperature.

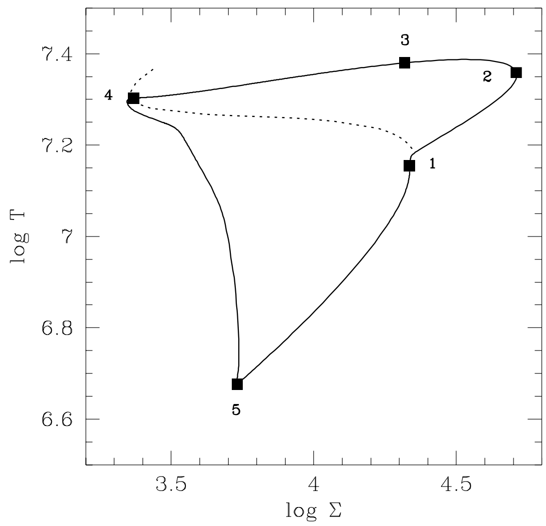

Figure 1. The phase portrait in the $\log T$-$\log \Sigma$ plane for $r = 10 r_G$ (here r_G is the Schwarzschild radius). The dotted line represents the equilibrium states, the so called S-curve. The lower branch of the S-curve overlaps with the trajectory of the evolving model. The continuous line shows the trajectory of the model during the evolution. The points marked 1 to 5 indicate those stages for which spectra are calculated. The points 1 to 4 correspond to the phase of disc evacuation, the point 5 is at the beginning of the refilling phase.

The first complete calculation of the global evolution of thermal instability in transonic discs was performed by Szuszkiewicz and Miller (1998). They have shown that at least for some values of M, $\dot{M}$ and α this evolution has a cyclic character and consists of successive evacuation and refilling phases. An example of the limit-cycle for the best studied thermally unstable model with $M = 10 M_{\odot}$, $\dot{M} = 0.06$ (in Eddington units) and $\alpha = 0.1$ is shown in Figure 1. This particular non-stationary disc behaviour might have interesting observational consequences.

2. Spectra in the blackbody approximation

The global dynamical calculations, described in Section 1, determine the overall properties of the transonic disc evolution. However, in order to get detailed theoretical predictions for the directly observed quantities, we must compute the spectra emitted from thermally unstable discs during the evacuation and refilling of their central parts. In the

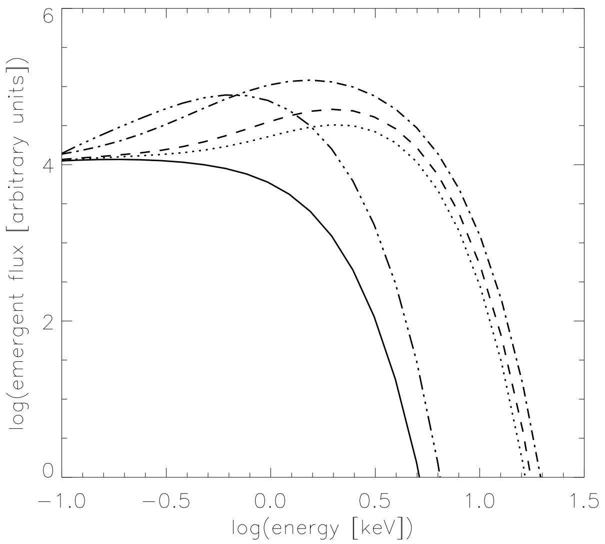

Figure 2. The disc spectra for the evolutionary stages shown in Fig. 1: stage 1 (solid line), stage 2 (dotted line), stage 3 (dashed line), stage 4 (dash-dotted line), and stage 5 (triple dashed-dotted line).

case of a geometrically thin accretion disc, it is possible to consider the vertical and radial disc structures separately. It is also reasonable to assume local heat balance. In order to calculate the spectrum, it is sufficient to divide the disc into a number of concentric annuli, calculate the spectrum emitted by each annulus and then sum them all together. The simplest assumption is that each annulus radiates like a blackbody at the local effective temperature. We stress that this assumption does not necessarily apply to all relevant physical situations. Most of the previous studies were concentrated on the modelling of the vertical structure and radiative transfer through each annulus in Shakura-Sunyaev discs (e.g. Shimura and Takahara, 1995). However, the thin disc hypothesis breaks down at high accretion luminosities and it may not be a good approximation at very low accretion rates either. Slim disc models are more appropriate for astrophysical applications (Szuszkiewicz et al., 1996; Wang et al., 1999). Here as a first approximation we have calculated spectra assuming that the disc radiates locally as a blackbody (Figure 2). During the disc evacuation phase the spectra become significantly harder. Detailed spectra calculations, which account properly for radiative transfer in the disc atmospheric layers are under way and will be presented in the forthcoming paper (Szuszkiewicz, Turolla and Zampieri, in preparation).

3. Concluding remarks

Transonic discs with accretion rates larger than a critical value which depends on the black hole mass and the viscosity parameter, show time dependent, cyclic behaviour due to the onset of thermal instabilities driven by radiation pressure. This behaviour can be described in terms of the cycle period, the duration of the bursting and quiescent phases, the amplitude and shape of the burst and finally by the spectral variability. For the different parameters of the system (M, α, $\dot{M}$) we expect different variability properties and emitted spectra. Detailed theoretical predictions are definitely needed for modelling high-resolution timing and spectral data presently available for black hole systems.

Acknowledgements

E.S. gratefully acknowledges financial support from the Polish State Committee for Scientific Research (grant KBN 2P03D01817), the Italian MURST and the University of Padova. Work partially supported through MURST grant COFIN9802154100.

References

Belloni, T., M. Mendez, A. R. King, M. van der Klis and J. van Paradijs. An Unstable Central Disk in the Superluminal Black Hole X-Ray Binary GRS 1915+105. *The Astrophysical Journal*, 479:L145–, 1997.

Shimura, T. and F. Takahara. On the spectral hardening factor of the X-ray emission from accretion disks in black hole candidates. *The Astrophysical Journal*, 445:780–788, 1995.

Szuszkiewicz, E., M. A. Malkan and M. A. Abramowicz. The Observational Appearance of Slim Accretion Disks. *The Astrophysical Journal*, 458:474–490, 1996.

Szuszkiewicz, E. and J. C. Miller. Limit-Cycle Behaviour of Thermally Unstable Accretion Flows on to Black Holes. *MNRAS*, 298:888–896, 1998.

Wang, J-M., E. Szuszkiewicz, F-J. Lu and Y-Y. Zhou. Emergent Spectra from Accretion Disks in Active Galactic Nuclei. *The Astrophysical Journal*, 522:839–845, 1999.

Disk–corona interactions in soft spectral states of black hole binaries

Piotr T. Życki
N. Copernicus Astronomical Center, Warsaw, Poland, (ptz@camk.edu.pl)

Abstract. Re-analysis of some archival X–ray data of black hole binaries in soft spectral states is presented. Results of detailed spectral fitting, including proper physical description of the X–ray reprocessed component, indicate that in most cases the soft, thermal disk emission cannot be described by a simple multi-color blackbody model. Additional Comptonization of those seed photons provides an acceptable description of the soft component, implying a presence of a warm ($kT_{\rm e} \sim 1$ keV), mildly optically thick ($\tau \sim 10$) phase of accreting plasma.

Combined spectral/temporal analysis of GS 1124-68 during 'flip-flop' transitions in VHS suggests that the optically thick accretion flow can proceed in (at least) two modes giving the same time-integrated behaviour (i.e. energy spectra) but very different timing behaviour.

Keywords: black hole, accretion disk

1. The Comptonized soft component

Accreting black holes, both stellar (including the Galactic μ–quasars) and supermassive, show strong, soft, thermal components in their EUV–X-ray spectra, when accreting above certain fraction of Eddington rate. This component is thought to come from an optically thick accretion disk, and its spectrum is usually modeled as a simple, multi-color blackbody. For re-examining a number of such spectra, I will use the spectral models described in Życki et al. (1998).

1.0. The Intermediate State

An example of IS is the May 18th observation of GS 1124-68 (Nova Muscae 1991). Using first the frequently employed but unphysical model, DISKBB + SMEDGE(POWERLAW), gives an unacceptable fit, $\chi^2_\nu = 38/25$. Adding a Gaussian line at 6.4 keV does *not* improve the fit, unless the line width is ~ 10 keV ($\chi^2_\nu = 28/23$). Allowing the line energy to be free gives $\chi^2_\nu = 21/23$ for $E = 4 \pm 0.5$ keV. These values have little to do with Fe spectral features, but rather indicate that it is the continuum shape that is not properly modeled. Using now the DISKBB + THCOMP + REL-REPR model gives very bad fit, $\chi^2_\nu = 308/24$. Replacing the DISKBB component with a Comptonized blackbody (COMPTT) results in a dramatic improvement, $\chi^2_\nu = 13/22$. Thus the best fit is obtained for the

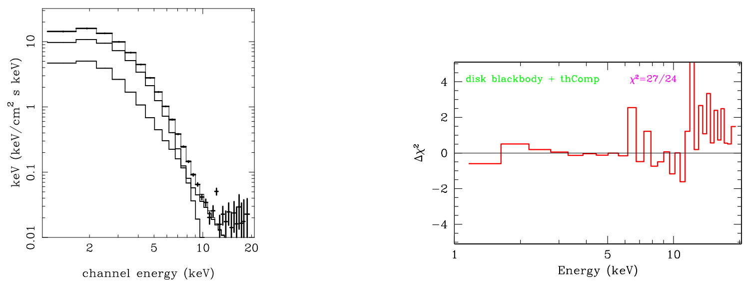

Figure 1. Spectrum of Nova Muscae 1991 in HS, showing a soft thermal component broader than a disk blackbody.

proper physical description of X–ray reprocessing and the *Comptonized blackbody* model for the soft component. The same effect is observed in GRO J1655-40, GS 2000+25 and XTE J1550-564 (Życki et al., in preparation).

1.0. The High State

Nova Muscae 1991 was in the High State when observed on Mar 18th. The spectrum shows a strong soft component, and the hard component is negligible (Ebisawa et al., 1994). Modeling the spectrum with the DISKBB + THCOMP model gives $\chi^2_\nu = 27/24$ (see Fig. 1). The Comptonized component is steep and makes a significant contribution to the soft component. Again, the soft component has to be described by a model *broader* than the multi-color disk blackbody.

1.0. The Very High State

On Jan 11th, while still on the rise to the peak of the outburst, Nova Muscae 1991, showed a spectrum consisting of two Comptonized components: the softer one again *cannot* be described by the DISKBB model. It can be modeled as Comptonization of ≈ 0.3 keV blackbody by a warm, $kT_{\rm e} \approx 3$ keV, optically thick, $\tau \sim 7$, plasma.

1.0. Physical origin of the Comptonization

The additional Comptonization seems to be a common feature of disk-dominated spectral states of accreting black holes. There are two possible scenarios to explain it. The first one is Comptonization in a "hot skin" on top of the accretion disk. Such a hot layer could not be heated by X–ray irradiation (as postulated for the low/hard state), but it would require enhanced viscous energy dissipation compared to the bulk of the disk. The second possibility is that the electron energy distribution in the Comptonizing plasma is a hybrid, thermal–non-thermal one, rather than a pure thermal (Maxwellian) distribution. In fact, the COMPPS model (J. Poutanen, private communication) using the hybrid distribution gives very good fits to the HS and IS data sets: $\chi^2_\nu = 17/24$ for IS, $\chi^2_\nu = 16/23$ for HS, but it fails for VHS.

2. Inner disk oscillations in GS 1124-68 in VHS?

Shortly before reaching the peak of outburst Nova Muscae 1991 showed 'flip-flop' transitions (Takizawa et al., 1997): the flux in the 2–20 keV band changed by $\approx$ 20%. Spectral and timing analysis during this period suggests that the source were undergoing re-structuring of the inner accretion disk.

2.0. Spectral analysis

Energy spectra both in the high- and low-flux state can be adequately described by the DISKBB + THCOMP + REL-REPR models (no additional Comptonization of the soft component is required). The best-fit model spectra differ most at energies 5–10 keV: the differences are small both at the lowest and highest energies (Fig. 2). The difference spectrum can be described as Comptonization of single blackbody emission, but it cannot be described as Comptonized *disk* blackbody.

2.0. Timing analysis

X–ray power density spectra show both energy and flux dependence. The soft X–rays ($E < 4$ keV) PDS is very different in the two flux states (Fig. 2). In the high flux state the PDS resembles that of typical HS, i.e. a power law $f^{-\alpha}$ with $\alpha \approx 1.2$, although there is also a narrow

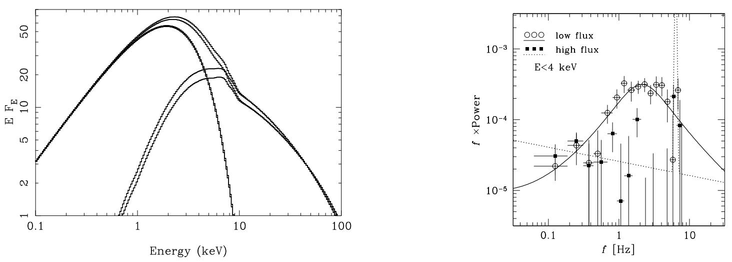

Figure 2. Energy and power spectra of Nova Muscae 1991 on Jan 14th (VHS), when the source showed 'flip-flop' transitions, probably related to re-structuring of the accretion disk. Two spectra in each panel are for two flux states.

QPO at ≈ 8 Hz. However, in the low flux state the PSD has a Lorenzian shape peaking (in the $f \times Power$ representation) at ≈ 2 Hz.

The PDS of the hard X–ray component ($E > 8.5$ keV) is similar in both flux states except for the QPO energy which is higher in the low flux state.

3. Discussion

Interactions between accretion disk and corona in the soft spectral states of accreting black holes are clearly complex. One outcome of those interactions is a presence of warm, mildly optically thick plasma modifying the disk thermal emission. Proper modeling of the resulting spectra is important e.g. for correct determination of system parameters.

The 'flip-flop' transitions observed in VHS of GS 1124-68 close to the peak of its outburst suggest that the optically thick accretion flow can proceed in two modes giving the same time-integrated characteristics. One mode, usually observed in HS, shows the f^{-1}-like PDS, i.e. a scale-invariant behaviour, perhaps realized in magnetic turbulence (Kawaguchi et al., 2000). The other mode clearly possesses certain spatial/temporal scale, since the PDS is described by a Lorenzian, i.e. it corresponds to exponential shots of a single time scale.

Acknowledgements

This work was supported in part by KBN grants no. 2P03D01816 and 2P03D01718.

References

Ebisawa, K. et al. Spectral evolution of the bright X-ray nova GS 1124-68 (Nova Muscae 1991) observed with GINGA. *P.A.S.J.*, 46:375–394, 1994.

Kawaguchi T. et al. Temporal $1/f^{\alpha}$ fluctuations from fractal magnetic fields in black-hole accretion flow. *P.A.S.J.*, 52:1-5, 2000.

Takizawa, M. et al. Spectral and temporal variability in the X-ray flux of GS 1124-683, Nova Muscae 1991. *Ap.J.*, 489:272–283, 1997.

Życki, P. T., Done, C. and Smith, D. A. Evolution of the accretion flow in Nova Muscae 1991. *Ap.J.Letter*, 496:L25-L28, 1998.

Inner Disk Oscillations and QPOs in Relativistic Jet Sources

A. R. Rao
Tata Institute of Fundamental Research, Mumbai, INDIA

Abstract. Recent results on the inner disk oscillations found in GRS 1915+105 are reviewed. QPOs during the low state are used as a marker for such oscillations and the physical picture emerging from a combined X-ray spectral and timing analysis is examined. The relationship between inner disk oscillations and synchrotron radio emission is critically evaluated.

Keywords: accretion, accretion disk, X-ray:stars, GRS 1915+105

1. Introduction

One of the remarkable features of the X-ray variability of the Galactic relativistic jet source GRS 1915+105 is the rapid intensity variations associated with repeatable and distinct spectral characteristics. Belloni et al. (1997) found that the source shows distinct and different inner disk radius during the "quiescence" and outburst which can be interpreted as the vanishing of the bright inner disk during the quiescence. Detection of rapid radio oscillations near the onset of superluminally moving ejecta prompted Fender et al. (1999) to suggest that such X-ray inner disk oscillations could be the underlying reason for the ejection of the synchrotron cloud responsible for the radio emission.

Ever since its discovery (Castro-Tirado et al. 1992) GRS 1915+105 has been exhibiting a rich variety of X-ray variability characteristics. Greiner et al. (1996) presented the RXTE observations of the source which included repeated patterns of brightness sputters, large amplitude oscillations, fast oscillations and several incidences of prolonged lulls. Belloni et al. (1997) classified some of the oscillatory X-ray variations as "outbursts" and from a time resolved spectral analysis found evidence for the disappearance of the inner disk during these oscillations. They also discovered a strong correlation between the quiescent phase and burst duration. Taam, Chen, and Swank (1997) detected a wide range of transient activity including regular bursts with a recurrence time of about one minute and irregular bursts. Paul et al. (1998) detected several types of such bursts using the IXAE data and found evidence for matter disappearing into the event horizon of the black hole. Yadav et al. (1999) made a systematic analysis of these bursts and classified them based on the recurrence time.

Belloni et al. (2000a) made a detailed evaluation of the X-ray variability characteristics of GRS 1915+105 and classified the variations in 12 different classes. To understand the basic nature of these classes, in Figure 1 we give the representative light curves and hardness ratios obtained from the *RXTE* archives. The total count rate, R, is in the units of 10^4 counts s^{-1} and it is vertically shifted by 5 units. The hardness ratio H1 (5 – 13 keV to 2 – 5 keV ratio) is scaled by 5 and shifted by 2 units and the hardness ratio H2 ($>$ 13 keV to 2 – 13 keV ratio) is scaled up by 10 and shifted by 4 units. The hardness ratio H1 is a measure of the disk blackbody temperature and H2 is a measure of the intensity of the hard power-law, presumably arising from a thermal-Compton cloud.

The X-ray variability classes which show steady behavior during one orbit of RXTE are shown in the top panel of the figure. Class ϕ is characterized by low count rate, low H1 and very low H2. It is also devoid of any strong variability. Class χ is characterized by strong 0.5 – 10 Hz QPO and it resembles the intermediate state of other black hole sources (Trudolyubov et al. 1999b). Classes δ, γ and μ are high-soft states of the source and occasionally the 67 Hz QPOs are seen in these states (Morgan et al. 1997).

The various X-ray variability classes which exhibit inner disk oscillations are shown in the middle panel of Figure 1. The distinguishing feature is the sharp ($<$ 10 s) change in the intensity state. During the high state of these oscillations the source exhibits all the temporal and spectral characteristics of the high-soft state of the source and during the low state it exhibits all characteristics of the low-hard state of the source (Rao et al. 2000b). The drastic change in H2, signifying a change in the Compton cloud, is a common feature of this class. The behavior can be regular (class ρ) and it can remain in this class for periods up to several tens of days. In class α the source reverts back and forth between class χ and class ρ. During the quiescent periods of all these classes the 0.5 – 10 Hz QPO is always present.

In contrast to such inner disk oscillations, classes ν, θ, and β show a more gradual change from a high-soft to low-hard state and they are characterized by a sharp soft dip when both H1 and H2 are low and the variability too drops to a low level. Radio oscillations are associated with these classes (Eikenberry et al. 1998; Mirabel et al. 1998).

2. Inner Disk Oscillations and QPOs

One of the remarkable features of the inner disk oscillations is the presence of the ubiquitous 0.5 – 10 Hz QPO during the quiescent state

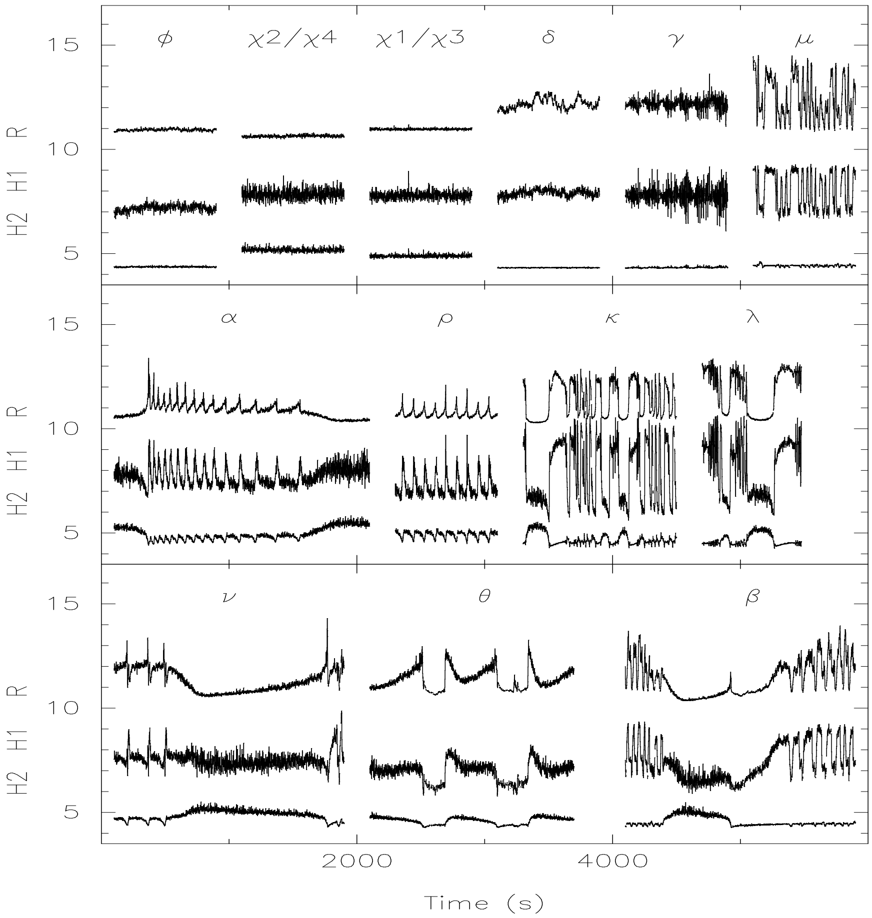

Figure 1. X-ray count rates (R) and the hardness ratios for the various classes of variability seen in GRS 1915+105.

of the oscillations. This type of QPO is found during the low-hard state of the source (and also in the low-hard state of other jet sources as well), and it is used as a marker for the low-hard state of the source (Muno et al. 1999; Trudolyubov et al. 1999b).

Reig et al. (2000) made a detailed study of the QPO phenomena in the $\chi 1$ and $\chi 3$ classes and found a correlation between the QPO frequency and the observed phase lag in the Fourier cross-spectrum in two energy channels. Nobili et al. (2000) have interpreted this correlation as due to arising from the geometry of the region producing the Compton spectrum, assumed to be arising from a corona formed by the puffed up inner regions of the accretion disk. Rao et al. (2000a) made a detailed spectral study during the $\chi 3$ state of the source and identified three spectral components. They found that the QPOs are due to the Compton component and they invoked an accretion disk shock to explain the QPO phenomena.

The large rms amplitude (about 10%), narrow width and the relative stability over considerably long durations makes it difficult to explain the 0.5 – 10 Hz QPO on the basis of any disk oscillation model. Chakrabarti & Manickam (2000) interpreted the QPOs as due to the oscillation of the region responsible for the hard radiation, i.e., the post-shock region. They also detected a correlation between the average frequency of the QPO and the duration of the 'off' states. A similar correlation with centroid frequencies were also found by Trudolyubov, Churazov, & Gilfanov (1999a).

There have been attempts to explain the rapid variability seen in GRS 1915+105 using disk instability models. Belloni et al. (1997) have tried to explain the repeated patterns as due to the appearance and disappearance of the inner accretion disk. Nayakshin et al. (1999) have investigated the different accretion models and viscosity prescriptions and attempted to explain the temporal behavior of GRS 1915+105. In particular, they have shown that the accretion instability in a slim disk is not likely to adequately account for the behavior of GRS 1915+105 (because of the difficulty in maintaining the high state for long) and the appearance of the inner accretion disk, as postulated by Belloni et al. (1997), will take a time scale comparable to the burst time scale. Though Nayakshin et al. (1999) were able to reproduce many characteristics in the X-ray variability for GRS 1915+105, they were unable to explain the rise/fall times or the < 10 s oscillations.

Yadav et al. (1999) presented a comprehensive picture for the origin of these bursts. They suggested that the peculiar bursts are characteristic of the change of state of the source. The source can switch back and forth between the low-hard state and the high-soft state near critical accretion rates in a very short time scale, giving rise to the irregular and quasi-regular bursts. It was pointed out that changes in total accretion rate cannot manifest itself in short time scales and hence the fast spectral state changes in GRS 1915+105 cannot be explained by changes in total accretion rates. Chakrabarti & Manickam (2000) provided an explanation for this remarkable observation by invoking mass loss. Unlike the canonical low-hard state where the hard power-law is due to Comptonisation, in the hard state observed during the bursts there should be an additional feature due to winds. Chakrabarti et al. (2000) have observed subtle differences in the spectra during the bursts compared to the spectra during the long duration low-hard and high-soft states. This change is above ~ 10 keV where the hard component of the low state softens. This is the effect predicted in Chakrabarti

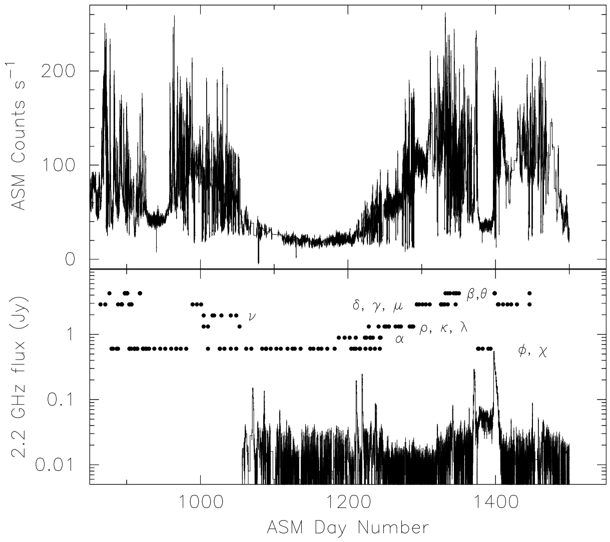

Figure 2. The ASM count rates for GRS 1915+105 is shown in the top panel and the 2.2 GHz GBI data is shown in the bottom panel. The time of occurrence of different intensity classes as established from the pointed RXTE PCA observations (Belloni et al. 2000a) are also shown in the bottom panel of the figure.

(1998) where the addition of about 10% mass loss in wind has an effect of pushing the spectral cross-over point from 15-17 keV (for a 10 $M_\odot$ black hole) to higher energies.

3. Inner Disk Oscillations and Synchrotron Radio Emission

There have been attempts to connect the X-ray variability characteristics to the onset of jet emission in GRS 1915+105. Fender et al. (1999) made a detailed analysis of the super-luminal jet ejection events observed in GRS 1915+105 in 1997 October/November and detected continuous short period (20−40 minute) radio oscillations during the start of the jet emission. They proposed that these are indications of repeated ejection of the inner accretion disk, quite similar to the events seen in X-rays by Belloni et al. (1997). A causal connection between disk and jet was thus attempted. Naik et al. (2000) have reported the detection of a series of X-ray dips during a huge radio flare of strength 0.48 Jy (at 2.25 GHz). They argue that a large number of such X-ray dips can account for the radio flare emission.

To put such disk-jet connections in perspective, we have shown in Figure 2 (top panel) the observed ASM count rates during 1996/1997. The concurrently obtained RXTE-PCA data have been classified by

Belloni et al. (2000a) and these are shown in the bottom panel of the figure, along with the 2.2 GHz radio data obtained from GBI public domain. The 1997 slow state transition is particularly interesting (see also Rao et al. 2000b).

It can be seen from the figure that the source was in a stable low-hard state up to 1997 April 25 (ASM day number 1210). The radio flux during this state is 20 – 30 mJy. This is the radio-quiet low-hard state of the source (Muno et al. 1999). The source started a steady increase in its X-ray emission with an average increase in the ASM count rate of 0.65 s^{-1} day^{-1} and reaching a count rate of 76 s^{-1} in the middle of July (day number 1290). During the beginning of the transition, the source showed several episodes of α states, accompanied by brief radio flares. For more than a month the source showed several episodes of the inner disk oscillations (classes ρ, κ and λ) (Yadav et al. 1999; Belloni et al. 1997). The source reached a steady high-soft state (classes δ, γ and μ) when the radio emission is very low (≤ 20 mJy). The ringing flares started again in the beginning of 1997 August (Yadav et al. 1999) and towards the end of this state the peculiar outbursts (class β) accompanied by infrared flares were observed on 1997 August 14-15 (Eikenberry et al. 1998). On September 9 the peculiar "outburst" was seen again (Markwardt et al. 1999). In October 1997 the source reached the radio-loud hard-steady state when both the X-ray and radio fluxes were high without the evidence of any oscillations. Fender et al. (1999) described this class as the "plateau" state.

From these we can conclude that the inner disk oscillations involving rapid transitions (classes ρ, κ and λ) do not lead to any appreciable radio emission. Apart from the radio-loud hard state, classes θ and β are associated with enhanced radio emission. Class β are associated with the synchrotron flares in radio (Mirabel et al. 1998; Fender & Pooley 1998) and infrared (Eikenberry et al. 1998). From simultaneous X-ray and infrared observations, Eikenberry et al. (1998) made a strong argument that the onset of radio/infrared flare is associated with the soft dip rather than the gradual change to the low-hard state. Radio oscillations on a time scale of $20 - 30$ minutes are seen to be accompanied by a series of soft X-ray dips (Fig. 10, Dhawan et al. 2000), similar to the oscillations observed by Fender et al. (1999). Since the soft dip events are associated with the jet emission, Naik et al. (2000) proposed that the huge radio flares are produced by a series of such soft X-ray dips.

Naik and Rao (2000) made a systematic study of the radio and X-ray emissions from GRS 1915+105 and found an one-to-one association between radio flares and the β and θ classes. If the onset of a huge radio flare (signifying the emission of a superluminal ejecta) is associated with an X-ray emission characteristic observed so far, it has to be necessarily with the β or θ classes. Belloni et al. (2000b), however, associate the change of state with the radio emission rather than the peculiar dips seen in these two classes. A continuous X-ray monitoring during a radio flare should clarify this question.

Acknowledgements

I thank the members of the RXTE and NSF-NRAO-NASA GBI team for making the data publicly available. This research has made use of data obtained through the High Energy Astrophysics Science Archive Research Center Online Service, provided by the NASA/Goddard Space Flight Center. I also thank S. Naik and S. V. Vadawale for helpful discussions and assistance in preparing this manuscript.

References

Belloni, T., M. Mendez, A.R. King, M. van der Klis and J. van Paradijs. An Unstable Central Disk in the Superluminal Black Hole X-ray Binary GRS 1915+105. *ApJ*, 479:L145–L148, 1997

Belloni, T., M. Klein-Wolt, M. Mendez, M. van der Klis and J. van Paradijs. A model-independent analysis of the variability of GRS 1915+105. *A&A*, 355:271-290, 2000a.

Belloni, T., S. Migliari, S. and R. P. Fender. Disk Mass Accretion Rate and Infrared Flares in GRS 1915+105. *A&A*, 358:L29–L32, 2000b.

Castro-Tirado, A.J., S. Brandt and N. Lund. *IAU Circ.*, 5590, 1992.

Chakrabarti, S. K. Spectral Softening Due to Winds in Accretion Disks. *Indian Journal of Physics*, 72B(6):565–569, 1998

Chakrabarti, S. K., S. G. Manickam, A. K. Nandi and A. R. Rao. Spectral Signature of Wind Formation from Post-shock Region in GRS 1915+105 Accretion Disk. *A&A*, submitted, 2000.

Chakrabarti, S. K. and S. G. Manickam. Correlation among Quasi-periodic Oscillation Frequencies and Quiescent-state Duration in Black Hole Candidate GRS 1915+105. *ApJ*, 531:L41–L44, 2000.

Dhawan, V., I. F. Mirabel and L. F. Rodriguez. AU-Scale Synchrotron Jets and Superluminal Ejecta in GRS 1915+105. *ApJ*, 543:373–385, 2000.

Eikenberry, S. S., K. Matthews, E. H. Morgan, R. A. Remillard and R. W. Nelson. Evidence for a Disk-Jet Interaction in the Microquasar GRS 1915+105. *ApJ*, 494:L61–L64, 1998.

Fender, R. P., S. T. Garrington, D. J. McKay, T. W. B. Muxlow, R. E. Spencer, A. M. Sterling and E. B. Waltman. MERLIN observations of relativistic ejections from GRS 1915+105. *MNRAS*, 304:865–876, 1999.

Fender, R. P. and G. G. Pooley. Infrared synchrotron oscillations in GRS 1915+105. *MNRAS*, 300:573–576, 1998.

Greiner, J., E. H. Morgan and R. A. Remillard. Rossi X-Ray Timing Explorer Observations of GRS 1915+105. *ApJ*, 473:L107–L110, 1996.

Markwardt, C.B., J.H. Swank and R.E. Taam. Variable-frequency Quasi-periodic Oscillations from the Galactic Microquasar GRS 1915+105. *ApJ*, 513:L37–L40, 1999.

Mirabel, I. F., V. Dhawan, S. Chaty, L. F. Rodriguez, J. Marti, C. R. Robinson, J. Swank and T. Geballe. Accretion instabilities and jet formation in GRS 1915+105. *A&A*, 330:L9–L12, 1998.

Morgan, E. H., R. A. Remillard and J. Greiner. RXTE Observations of QPOs in the Black Hole Candidate GRS 1915+105. *ApJ*, 482:993–1010, 1997.

Muno, M. P., E.H. Morgan and R. A. Remillard. Quasi-periodic Oscillations and Spectral States in GRS 1915+105. *ApJ*, 527:321–340, 1999.

Naik, S. and A. R. Rao. Disk−jet connection in GRS 1915+105: X-ray soft dips as cause of radio flares. Â&A, in press, astro-ph/0008433, 2000.

Naik, S., P. C. Agrawal, A. R. Rao, B. Paul, S. Seetha and K. Kasturirangan. Detection of a Series of X-ray Dips Coincident with a Radio Flare in GRS 1915+105. *ApJ*, in press, astro-ph/0008414, 2000.

Nayakshin, S., S. Rappaport and F. Melia. Time-dependent Disk Models for the Microquasar GRS 1915+105. *ApJ*, 535:798–814, 2000.

Nobili, L., R. Turolla, L. Zampieri and T. Belloni. A Comptonization Model for Phase-Lag Variability in GRS 1915+105. *ApJ*, 538:L137–L140, 2000.

Paul, B., P. C. Agrawal, A. R. Rao, M. N. Vahia, J. S. Yadav, S. Seetha and K. Kasturirangan. Quasi-regular X-Ray Bursts from GRS 1915+105 Observed with the IXAE: Possible Evidence for Matter Disappearing into the Event Horizon of the Black Hole. *ApJ*, 492:L63–L66, 1998.

Rao, A. R., S. Naik, S. V. Vadawale and S. K. Chakrabarti. X-ray Spectral Components in the Hard State of GRS 1915+105: Origin of the 0.5 - 10 Hz QPO. *A&A*, 360:L25–L29, 2000a.

Rao, A. R., J. S. Yadav and B. Paul. Rapid State Transitions in the Galactic Black Hole Candidate Source GRS 1915+105. *ApJ* in press, astro-ph/0007250, 2000b.

Reig, P., T. Belloni, M. van der Klis, M. Mendez, N. D. Kylafis and E. C. Ford. Phase Lag Variability Associated with the 0.5–10 Hz Quasi-Periodic Oscillations in GRS 1915+105. *ApJ*, 541:883–888, 2000

Taam, R. E., X. Chen and J. H. Swank. Rapid Bursts from GRS 1915+105 with RXTE *ApJ*, 485:L83–L86, 1997.

Trudolyubov, S., E. Churazov and M. Gilfanov. The 1–12 Hz QPOs and Dips in GRS 1915+105: Tracers of Keplerian and Viscous Time Scales ? *A&A*, 351:L15-L18, 1999a.

Trudolyubov, S., E. Churazov and M. Gilfanov. The X-ray source GRS 1915 + 105: The low-luminosity state and transitions between the states during 1996-1997 (RXTE observations). *Ast. L.*, 25:718–738, 1999b.

Yadav, J. S., A. R. Rao, P. C. Agrawal, B. Paul, S. Seetha and K. Kasturirangan. Different Types of X-ray Bursts from GRS 1915+105 and Their Origin. *ApJ*, 517:935–950, 1999.

Chasing the Instability:
Spectral and Timinig Analysis of GRS 1915+105

S. Migliari[1,2], F. Vignarca[1,3], T. Belloni[1]
[1] *Osservatorio Astronomico di Brera, Merate (LC), Italy*
[2] *Dipartimento di Fisica, Università degli studi di Milano, Milano, Italy*
[3] *Dipartimento di Scienze, Università dell'Insubria, Como, Italy*

Abstract. The superluminal galactic microquasar GRS 1915+105 shows complex variability in the X-ray band. This has been interpreted as an instability of the inner region of an optically-thick accretion disk. Making use of RXTE/PCA data, we inspected in detail the instability intervals of the source. We concentrated upon the light curves for which the disappearance of the inner region lasts sufficiently long to trace the behaviour of single parameters. Fits of time-resolved power spectra yielded the parameters of the 1-10 Hz QPO, while time-resolved energy spectra allowed us to find the disk inner radius and temperature, and the power-law photon index during the evolution of the instability. We present the analysis of the parameters and their correlations and discuss them in terms of current accretion disk models.

Keywords: accretion, accretion disk, close binaries, X-ray:stars, GRS 1915+105

1. Introduction

The BHC GRS 1915+105 is an extremely variable X-ray transient which shows superluminal jets in the radio. The large variability in the X-ray band is compatible with the oscillations of the inner region of the accretion disk around the black hole (see Belloni et al. 2000). Our aim is to follow in more detail the evolution of spectral and timing parameters during the instability intervals (see Belloni, this volume).
We analyzed RXTE/PCA data of selected GRS 1915+105 observations, corresponding to classes α, β, ν, κ and λ as in the classification by Belloni et al. (2000), in which the instability intervals last sufficiently long to trace the evolution of spectral and timing parameters. We isolated long low-flux intervals corresponding to states C and A (Belloni et al. 2000). For each interval, we produced energy spectra with an integration time of 16 s and fitted each spectrum using the "standard" model for BHCs, consisting of the superposition of a multicolor disk-blackbody and a power-law. From the same data, we extracted power spectra of selected intervals of 4 and 16 seconds. We fitted these power spectra, using Lorentzian functions, in order to find the characteristic frequency of the QPO in the 1-10 Hz frequency range.

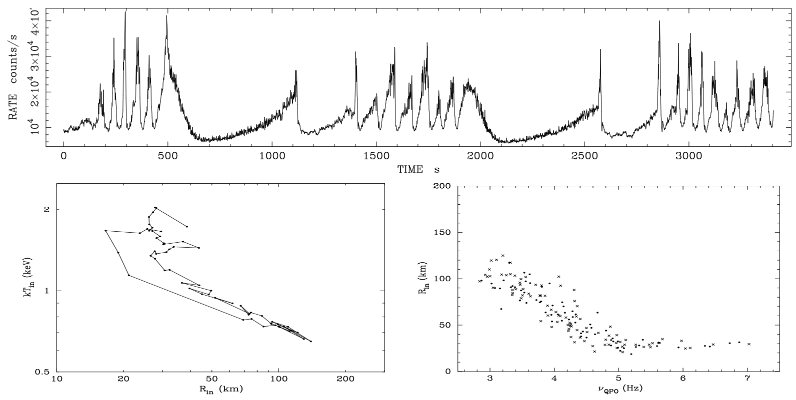

Figure 1. Top: PCA light curve of GRS 1915+105 corresponding to class β. Left: Correlation between inner disk radius and temperature during the instability of the accretion disk. Right: Correlation between QPO frequency and inner radius for many instability intervals.

2. Results

After obtaining the spectral and timing parameters, we investigated their behaviour by first following the time evolution of single parameters and then linking them to each other. Correlations between spectral parameters ($\mathrm{kT}_{in} - \mathrm{R}_{in}$, $\mathrm{kT}_{in} - \Gamma$, $\mathrm{R}_{in} - \Gamma$) yield constraints for more detailed instability models. Figure 1 (left panel) shows an example of a $\mathrm{kT}_{in} - \mathrm{R}_{in}$ evolution plot during a β-class instability. An important aspect of accretion disk physics is the connection between disk accretion and jet ejection. We can investigate in more detail this connection, comparing disk parameters and jet features from mutiwavelength observations in Radio, IR and X-ray band (see Klein-Wolt et al., this volume). Other results are found when correlating QPO frequencies, obtained from timing analysis, and inner radii, obtained from spectral analysis. It is evident (Figure 1, right panel) that the 1-10 Hz QPO is strictly linked to the status of the accretion disk. Moreover, a correlation is also found between QPO frequency and power-law index Γ, showing that the power-law component is important for the origin of QPO. Our analysis shows that only by taking into account both spectral and timing parameters we have a complete picture of the complex phenomenology of GRS 1915+105.

References

Belloni et al., A model-indipendent analysis of the variability of GRS 1915+105, A&A, 355, 271 (2000)

Thermal Comptonization in GRS 1915+105

Osmi Vilhu and Petter Nikula
Observatory, Box 14, FIN-00014 University of Helsinki, Finland

Juri Poutanen
Stockholm Observatory, SE-133 36 Saltsjöbaden, Sweden

Jukka Nevalainen
ESA/ESTEC Astrophysics Division

Abstract. The Rossi X-ray Timing Explorer (*RXTE*) data of GRS 1915+105 from several observing periods were modelled with a thermal Comptonization model. In the model (Fig. 1), seed soft photons from an optically thick cool disk are Comptonized in a hot spherical corona surrounding the inner disk. Although the coronal temperature and optical depth can not be determined simultaneously, a qualitative trend was observed: At high soft states the inner disk just touches the outer edge of the central corona, while during low hard states the corona is larger and denser and surrounds the inner disk.

1. Introduction and Results

The X-ray transient GRS 1915+105 was discovered by Castro-Tirado et al. (1992) using WATCH all-sky monitor on the GRANAT satellite. Since then it has been an active X-ray source with superluminal jets found by Mirabel and Rodriquez (1994). The *Rossi X-ray Timing Explorer* (*RXTE*) has been monitoring it frequently and a rich pattern of variability has emerged from these data (see Belloni et al, 2000; Vilhu and Nevalainen, 1998; Muno et al. 1999). We collected several Proportional Counter Array (PCA) and High-Energy X-ray Timing Experiment (HEXTE) observations of GRS 1915+105, performed during 1996-97, from the TOO-archive of *RXTE*, and modelled the spectra with a thermal Comptonization model in a specific sombrero-geometry.

In the model (Fig. 1), the disk penetrates into the central spherical coronal region with electron temperature kT_e, Thompson optical depth τ and coronal radius R_{cor}. The optically thick multi-temperature disk, with inner disk radius R_{in}, radiates the observed soft spectrum and serves as the source of seed photons for Comptonization in the corona. Inside the corona the disk temperature was assumed constant. The radiative transfer in the corona was handled by the iterative scattering method developed by Poutanen & Svensson (1996) and incorporated into the XSPEC spectral fitting software.

The results are shown in Fig. 2 where the coronal temperatue was fixed to 70 keV (T_e and τ can not be determined separately, only

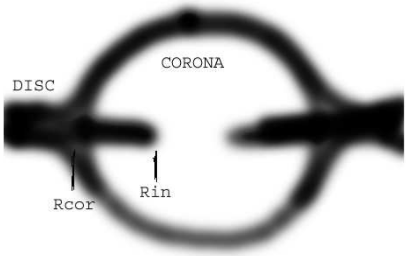

Figure 1. The Sombrero-model geometry

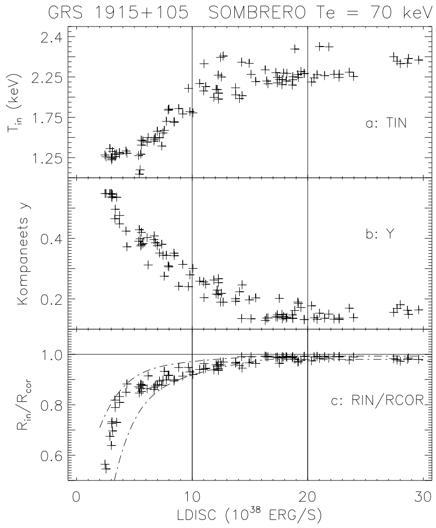

Figure 2. Model parameters as a function of the disk luminosity

their product, the Kompaneets y-parameter, is well defined by the observations). However, the following trend is at least qualitatively independent on this assumption: *At high soft states the inner disk just touches the outer edge of the central corona, while in the low hard states the corona is larger and denser and totally surrounds the inner disk.*

References

Belloni, T., Klein-Volt, M., Mendez, M., et al. 2000, AA 355, 271
Castro-Tirado, A. J., Brandt, S., & Lund, N. 1992, IAU Circ. 5590
Mirabel, I. F., & Rodriquez, L. F. 1994, Nature 371, 46
Muno, M. P., Morgan, E. H., & Remillard, R. A. 1999, ApJ 527, 321
Poutanen, J., & Svensson, R. 1996, ApJ 470, 249
Vilhu, O., & Nevalainen, J. 1998, ApJ 508, L89.

Nonlinear time-series analysis of the X-ray flux of compact objects

M. Thiel, M. Romano, U. Schwarz and J. Kurths
Universität Potsdam

G. Hasinger
AIP Potsdam

T. Belloni
Astronomical Institute "Anton Pannekoek", University of Amsterdam

Abstract. We analyse the X-ray light curves of compact objects using linear and nonlinear time series analysis methods. A Power Density Spectrum (PDS) describes the overall second order properties of the observed data well. To look beyond we propose the nonlinear Q-statistic to detect an asymmetry of the time series. This allows us to find relevant time scales. This method even grants a subclassification of the known states of X-ray sources.

Keywords: X-ray variability, Cyg X-1

1. Q-Statistic

We consider the nonlinear quantity "asymmetry in time" $Q(m)$ of the set of data x_k, corresponding to an irreversibility in time, to characterize the observation beyond linearity (Timmer et al. 2000). The significance $S(m)$ of this quantity $Q(m)$ corresponding to the null hypothesis of a linear Gaussian process is computed by the method of surrogate data (Kantz & Schreiber 2000). The general idea is to simulate time series whose statistical properties are constrained to the null hypothesis one wants to test for. In testing for a linear Gaussian process (colored noise) we randomize the phases of the Fourier Transform of the data and transform the modified series back to the time domain.

2. Results for Cyg X-1 / Conclusions

We analyze the X-ray flux of Cyg X-1 in each low-, high- and intermediate state. The data are recorded on various days with the PCA on board the RXTE. The energy range is 2.0 - 14.1 keV. The sampling frequency is 256 Hz. The data sets consist of 100,000 points. Applying the Q-statistic to the observational the data, we get a graphical representation of both $Q(m)$ (left panel) and $S(m)$ (right panel) of an low- an intermediate- and a high-state:

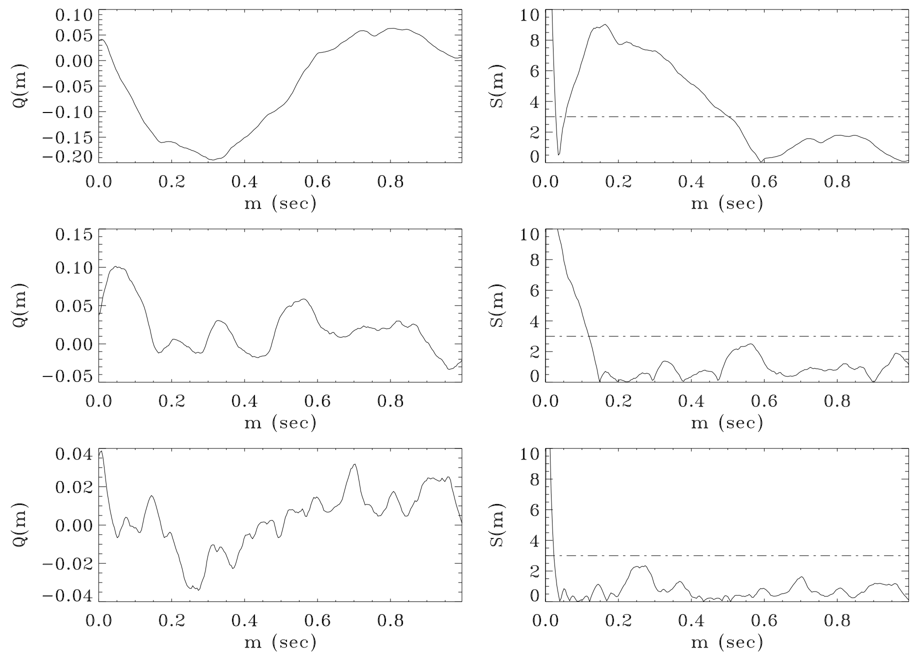

Figure 1. $Q(m)$ and $S(m)$ of low-, intermediate- and high-state (top to bottom)

Even though we have not yet a phyiscal interpretation of the structures in $S(\tau)$ and $Q(\tau)$, the results have some striking points: i) Changes of both $Q(m)$ and $S(m)$ in the low states occur on larger time scales than in the other states. ii) The decay of the first peak of $S(m)$ in an intermediate state is about double time as in the other two states. iii) The peaks of $Q(m)$ and $S(m)$ are anticorrelated in the low- and high- but correlated in the intermediate state. iv) The fine structure allows a subclassification of the different states of Cyg X-1. v) As we will show there is a close relationship between Fourier coefficients and the Q-statistics, (Thiel et al. 2000). vi) The Q-statistic provides information about the time-series that a PDS cannot discover.
Our next step is to try to connect physical processes, e.g. turbulence, to the structures of $S(\tau)$ and $Q(\tau)$, (Thiel et al. 2000).

References

Timmer, J., Schwarz, U., Voss, H.U., Wardinski, I., Belloni, T., Hasinger, G., van der Klis, M., Kurths, J.: 2000,*Phys.Rev.E*\ **61**, pp. 1342-1352

Kantz, H., Schreiber, T.:1997, 'Nonlinear time series analysis',*Cambridge University Press*

Thiel, M., Romano, M., Schwarz, U., Kurths: to be published